Self-assembled nanostructures as templates for patterned surfaces with non-microelectronic applications

J. Kerry[a], T Ghoshal[a,b] and M A Morris[a,b,*]

[a]Departments of Chemistry and Food Science and Technology, University College Cork, Ireland; [b]AMBER, Trinity College Dublin, Ireland

ABSTRACT

This paper outlines alternative uses of block copolymer (BCP) patterning compared to their well-researched exploitation in defining silicon circuitry and interconnects. The challenge in these alternative applications is usually to define 'active' patterns of materials other than silicon and instead of using the self-assembled block copolymer pattern as a means to form an on-chip etch mask, to use it as a template for deposition of functional components. In this paper we briefly discuss progress in the field of block copolymer patterning and some potential applications. The paper will then outline two examples in the area of sensing and antimicrobial surfaces. Here, polystyrene-b-polyethylene oxide (PS-b-PEO) is used as a suitable template as it forms well-ordered arrangements on several substrate types. The PEO block can then be used as a host block towards precursor inclusion from solution because of its' selective chemistry. Onward processing then creates a pattern of included materials that mimics the original BCP arrangement. To demonstrate the potential of these methods we illustrate examples as sensors and antimicrobial surfaces which both take advantage of the small feature size, high surface area and coverage that can be attained by these techniques.

Keywords: Block copolymer, patterning, precursor inclusion, nanodots, sensors, antimicrobials

1. INTRODUCTION

Bottom-up, chemical nanopatterning, nanophase separation, all common expressions amongst a myriad of terms used to describe potential techniques for how surfaces and substrates can be nanoengineered without the use of physical methods such as lithography.[1] The hope of being able to create surface arrangements of precise periodicity and dimension has been around since the original papers on self-assembly (and the quite distinct self-organization) which described how molecular and physical entities can spontaneously organize themselves into regular arrangements through intermolecular forces.[1] Despite the promise of this approach there are relatively few examples where self-assembly has had a real impact in a commercial sense. One clear example has been the development of mesoporous materials that are manufactured for chromatography and sorption applications.[2]

However, self-assembly has been closely associated with nanotechnology and, in particular, the development of nanosized electronic devices. Whilst considerable progress has been achieved and key capability demonstrated, the goal of having arrays of devices formed by self-assembly has yet to be achieved.[3] There are many reasons for this; integration (effectively placement) of the individual devices into the true circuitry is a challenge, reproducibility and reliability of the methods is an issue and, of course, defectivity over large substrates areas is an inherent problem of all forms of self-

*m.morris@ucc.ie; phone 00353 21 4902180; fax 00353 21496 2074

assembly because of its statistical nature.[4] However, one form of self-assembly/organization is moving towards device manufacture and inclusion into sub 8 nm technology nodes is become ever more probable.[5] Block copolymer (BCP) lithography is becoming a viable, scalable and realizable method for line space (interconnects, devices) and hole (via) patterning at ultra-small feature sizes.[6,7] Here, using techniques such as grapho- and chemi- epitaxy, the microphase separation of BCPs can achieve extremely ordered arrangements through chemical interactions between the constituent polymer blocks. The polymer patterns can be integrated into current fabrication schemes as a non-UV lithographic on-chip etch mask provided one block in the pattern can be selectively removed. Brief examples of the progress in this area are illustrated in Figure 1.

The work in BCP nanolithography has been driven by the challenges (both financial and technical) in providing sub 8 nm feature size resolution in transistor circuitry and has dominated the academic and industrial research in this area.[5-7] However, we have learned a great deal about how these patterns can be achieved, morphology and structural control as well as choices of polymers and how a range of materials can be realized.[6,7] Despite the considerable progress that has been made, outside their uses in nanoelectronic fabrication, their applications in fields that require patterning of sub 50 nm feature size in a range of materials has been somewhat neglected despite their low cost.
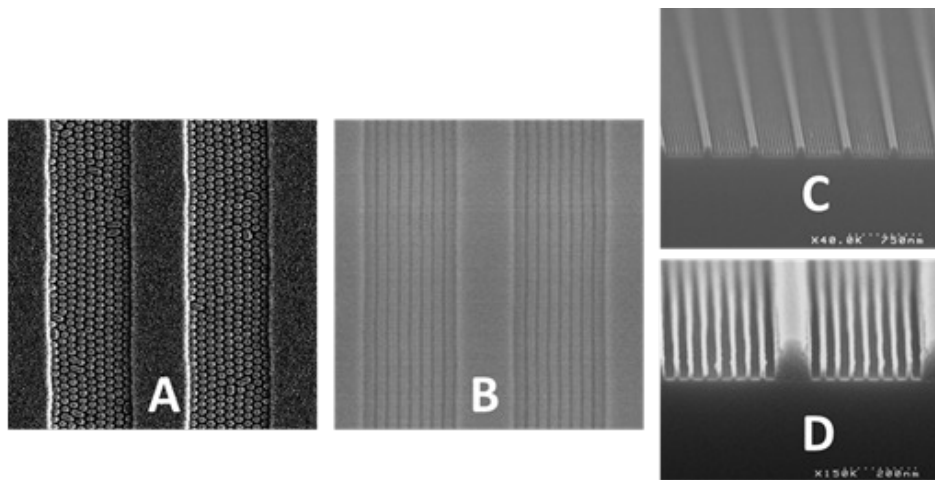

Figure 1. Typical block copolymer patterns formed in topographically patterned surfaces. A and B represent vertical and parallel orientation of hexagonal cylinder forming polystyrene-b-polydimethylsiloxane. C and D represent silicon structures formed by pattern transfer of similar arrangements to B (with permission of author and M. Zelsmann, LTM-CNRS, Grenoble, France)

However, moving these materials and processes from the microelectronic fabrication towards a more general method of surface nanoengineering across a range of material and substrate types will require considerable effort. The requirement for absolute precise positioning, defectivity and dimensional regularity defined by circuitry are, of course, somewhat reduced. Nonetheless, the generation of functional nanopatterns using block copolymers will not be facile and instead a series of new challenges emerge. We can relatively easily define some of these:-

a)   realizing patterns in a range of possible material sets (from extension to novel semiconductors such as germanium, III-Vs through to metal oxides, metals and even emerging 2D materials such as graphene),
b)   extension to other substrates such as glass, polymer, metal including flexible and packaging surfaces,
c)   developing routes around low capital investment requirements that allow fabrication at scale and low cost without use of e.g. UV lithography and expensive cleanroom techniques,
d)   using these materials to generate patterned functionality that exceed current performance at acceptable cost.

These materials might generate functional nanopatterned applications in a number of ways. The schematic in Figure 2 illustrates some of the most important of these and are discussed in further detail below. In Figure 2A, one or more

polymer blocks consist of either blocks that can be readily removed to create designed nanoporosity or one or more of the blocks are themselves functional (liquid crystals or fluorescent materials). A possible application is where the polymer structure acts as a photonic crystal and can be used to create a colorimetric solvent sensor device as the properties of the BCP are changed.[8] This is a simple device concept that combines the periodic arrangement of the block copolymer with the inherent ability of polymers to swell in selected solvents and so change periodicity. TiO_2 is selectively impregnated into one block to provide refractive index contrast and so color sensitivity. One might imagine similar applications in pH and size selective molecular determination. Probably the most well-developed area is where one block is selectively removed (e.g. by designing easily cleavable links between the blocks[9]) to create a nanoporous film or membrane as described in top of Figure 2B. The formation and structure of these has been detailed elsewhere and they have applications in size selective filtration, particle growth and even selective crystal phase development.[10] A related but somewhat different interesting application of block copolymer films is as superhydrophobic surfaces.[11] Here, the nanosized structure and inherent polymer hydrophobicity combine to give surfaces which will not wet and have applications in areas such as anti-biofouling surfaces.
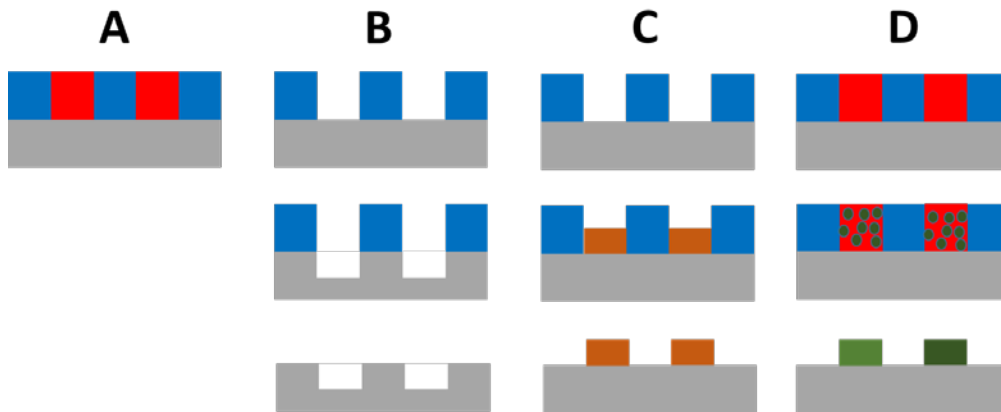

Figure 2. Methods of producing nanoscale features in materials (see text for details). A – active polymer patterning, B – pattern transfer to a substrate, C – templating and D – infill or impregnation methods.

Of course, any suitable BCP that generates the required pattern at a substrate surface and has sufficient etch contrast between the blocks exists can be used in the form of pattern transfer described in Figure 1.[12] The method is shown schematically in Figure 2B. Briefly, one block is selectively removed to yield a topographical etch mask which then protects the substrate during an etch process. Small feature size topography in silicon substrates has been used to create electrochemical ethanol sensors in this way[13]. Figure 2C illustrates a classic template type reaction where material is deposited into the topography. Removal of the remaining polymer or lift-off yields the final structure. This type of technique has been used to create copper based capacitors by depositing metallic copper into polystyrene templates created from the polystyrene-b-polymethylmethacrylate system.[14] In Figure 2D, one block is selectively modified by inclusion of a desired component or a precursor thereto. Removal of the polymer and modification of the precursor yields the final structure. Examples of this methodology will be described in detail below to show how this can be used to prepare well-defined nanodot arrangements. Two exemplars of the possible applications of these systems will be discussed.

2. EXPERIMENTAL

2.1 Preparation of iron oxide and silver nanodots

The polystyrene-*block*-poly(ethylene oxide) (PS-*b*-PEO) BCP is an excellent example of a readily impregnated system. The PS block is highly hydrophobic whilst PEO can be relatively easily swollen using hydrophilic and polar molecules such as ethanol. We have described the methodology previously.[15,16] Hexagonal arrangements of PEO cylinders within

a PS matrix can be readily created from asymmetric BCPs and in suitable process conditions, these arrangements can be formed across large areas with a vertical arrangement of cylinders and by inclusion from a solvent, precursors can be selectively included into the PEO block (as Figure 2D). A range of molecular weights can be used to control the size and spacing of the nanodots and we have used PS-b-PEO with relative block weights of M_n = 32-11, 42-11.5 and 102-34 kg mol^{-1} (polydispersities ~1.05) where, M_n is the number-average molecular weight. These were purchased from Polymer Source Inc., Canada. Because of the limited space available in this article we will use exemplars as being indicative of the range of polymers used. Nanodots were formed in the following way. BCPs were dissolved in toluene and after ageing (12 h) this solution was spin-coated onto substrates at 3000 rpm for 30 s. The films were solvent annealed in toluene or toluene/water at 50 ^{o}C for about 1 h, the exact conditions varied for each system to give the optimum film structure and morphology. Although the microphase separated films can be directly exposed to precursor solutions this does not yield the best quality nanodots and overfill and poor shape/size control result. Instead, partial etching and domain modification of PEO was carried out by ultrasonication of the films in anhydrous alcohol for optimized time periods. Following drying, ethanolic solutions of metal salts (here $Fe(NO_3)_3,9H_2O$ and $AgNO_3$) were spin-coated onto the modified BCP films. UV/Ozone treatment was used to oxidize the precursor and remove polymer as shown in Figure 2D.

The substrates used where either ITO coated glass substrates (with surface resistivity of 8-12 Ω/m^2 and coating thickness of 120-160 nm) or conventional microscope slides, both purchased from Sigma-Aldrich. Prior to coating these were cleaned by ultrasonication in ethanol and toluene for 30 min each and dried under a nitrogen stream. The quality of the films and nanodots were similar on these and other substrates including silicon, quartz, alumina, silicon nitride, etc.

2.2 Characterization

Surface morphologies were imaged by scanning probe microscopy (SPM, Park systems, XE-100) in tapping mode and scanning electron microscopy (SEM, FEI Company, FEG Quanta 6700). The Transmission Electron Microscope (TEM) lamellae were prepared by a Zeiss Auriga-Focused Ion Beam (FIB) cobra ion column having 2.5 nm resolution and analyzed by an FEI Titan-TEM operating at an accelerating voltage of 130 kV. Compositional analysis was investigated by energy dispersive x-ray analysis (EDAX). Film thicknesses were measured by optical ellipsometery (Woolam M2000) and electron microscopy. X-ray photoelectron spectroscopy (XPS) experiments were conducted on a Thermo K-alpha machine with an Al K$_\alpha$ x-ray source operating at 72 W. Crystallinity of the nanodots was examined by X-ray diffractometer (XRD, PANalytical MPD) using an Xcelerator detector and a Cu K$_\alpha$ radiation (45 kV/40 mA).

2.3 Antimicrobial Activity.

The antimicrobial activity of the Ag nanodots was assessed against pure cultures of *P. fluorescens* (NCIMB 9046) and *S. aureus* (NCIMB 13062). Both bacteria were grown in Muller-Hinton broth (MHB) for 18 h at 30 or 37 °C for *P. fluorescens* and *S. aureus,* respectively, under constant agitation on an orbital shaker at 170 rpm. Final bacterial load of *P. fluorescens* and *S. aureus* were 1.8 x 10^9 and 2.3 x 10^9 colony forming units per milliliter of culture (CFU/ml), respectively. For diffusion-type assay methods Muller-Hinton agar (MHA) plates were swabbed with the working culture bacteria (grown bacteria for 18 h, diluted in MHB to ~10^6 CFU/ml). Before use, the glass slides were exposed to UV light for 15 min in a laminar flow (Airclean 600 PCR Workstation STAR LAB). The glass slides were then placed in the middle of the inoculated agar plates and incubated for 24 h at 30 °C or 37 °C, for *P. fluorescens* and *S. aureus,* respectively. Blank (control glass slides without Ag nanodots) was also tested as negative controls. The inhibition halo formed around the substrate was recorded as an indication of inhibition against the bacteria tested and measured using an electronic calliper (Model ECA 015D Moore &Wright, Paintain tools Ltd., Birmingham, UK) in millimeters.

2.4 Electrochemical Measurements

The electrochemical experiments were undertaken in three electrode setup of VersaSTAT 3 (Princeton Applied Research, USA) potentiostat tool that includes VersaStudio software. Ag/AgCl and KCl formed the reference electrode and platinum wire acts as counter electrode. Prior to experiments solutions were de-aerated by bubbling nitrogen for 30 min at (293K ± 1) K. The cyclic voltammetric curves for electro-oxidation of EtOH and H_2O_2 (30.0%) were measure in a 0.5 M phosphate buffer solution (pH = 7.4).

3. RESULTS

3.1 Nanodot Formation

Illustrative tapping mode AFM images of PS-b-PEO (32-11 and 42-11.5) after spin-casting onto ITO and solvent annealing are shown in Figure 1a and 1c. The patterns are typical of hexagonally arranged PEO cylinder microdomains in the PS matrix. The PEO cylinders were seen darker in colour where PS, the major component in lighter contrast constitutes the matrix. The films extend across the substrate surface and are of regular thicknesses of 25 nm and 40 nm for the 32-11 and 42-11.5 PS-b-PEO cylinders respectively. The corresponding measured average cylinder centre to centre distances are 32 nm and 42 nm, respectively, whereas the PEO cylinder diameters were 17 nm and 19.3 nm, respectively. The strong multiple peaks in the FFT pattern shown in the insets of the Figures 1a and 1c confirm highly ordered hexagonal arrangement of PEO cylinders.
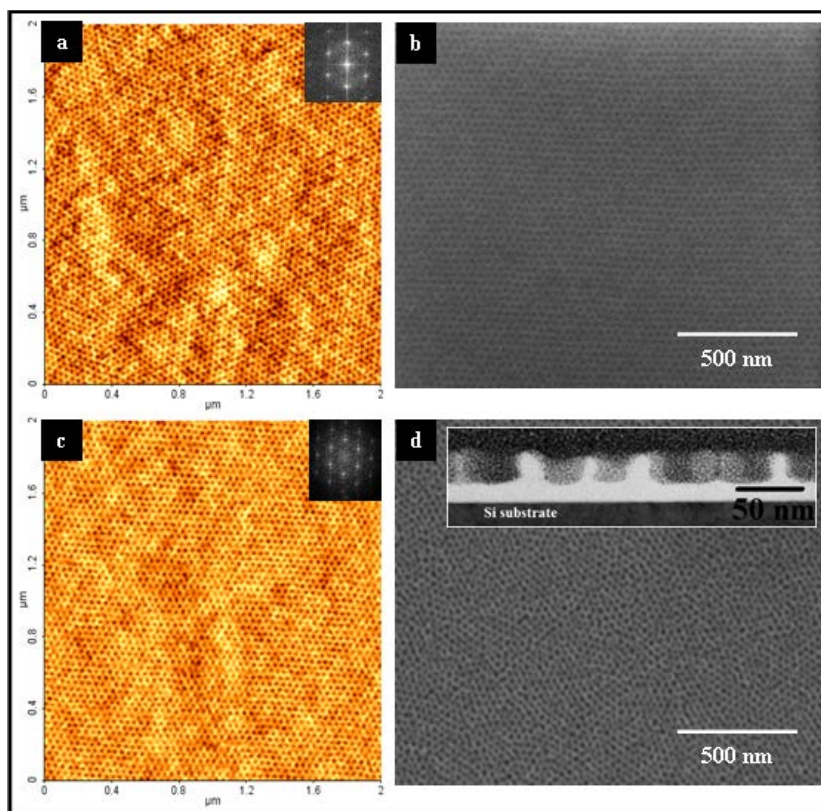

Figure 3. AFM (a and c) and SEM images (b and d) of well-arranged BCP patterns on ITO after solvent annealing. Upper images are from PS-b-PEO 32-11 and lower 42-11.5. Insets of a and c are FFT of the images revealing the highly ordered hexagonal arrangement. The inset of d is a cross-section revealing the porosity achieved after ethanol treatment of the original phase separated systems.

The ultrasonication of these films in ethanol is important in defining the maximum fidelity of the nanodots patterns with the original BCP arrangement. It is clear that this treatment (carefully optimized) does not remove all of the PEO in the film but rather partly removes the PEO creating free volume (as nanoporosity) but maintaining a PEO coating of the PS walls.[15,16] Figures 3b and 3d shows the SEM images of the PS-*b*-PEO systems after ethanol treatment for 15 min and 17 min for sample A and B, respectively. That these films can be readily imaged using SEM (i.e. block contrast has been enhanced significantly) is consistent with removal and pore formation. Note that longer exposure to ethanol and higher temperatures resulted in surface roughness or structural degradation of the film. Presumably, the reduction in the optimal ethanol treatment time as molecular weight decreases is related to reduced mass transport limitations at smaller dimensions. No film thickness changes were observed by ellipsometery. The cross-section TEM (Figure 3d inset) of the films confirms the nanoporosity after these ethanol treatments. As mentioned above this film structure is ideal as the

porosity enhances filling by capillary forces whilst residual PEO swell and 'absorbs' the precursor and solvent. It might be conjectured that the pore volume created also prevents over-swelling of the PEO cylinders across the surface and, as a result, the nanodots are very well-defined by the PS matrix.

Iron oxide nanodots were formed by the inclusion of the metal ions into the nanoporous template *via* spin coating of an ethanolic solution (0.4 wt % precursor solution) as above and subsequent UV/Ozone treatment. Figures 4a and 4c show the SEM images of well-ordered iron oxide nanodots arrays formed after UV/Ozone treatment with the templates for PS-b-PEO 32-11 and 42-11.5 respectively. The nanodots have uniform size, shape and their placement mimics the original self-assembled BCP patterns. The average diameters of the nanodots were 18 nm and 24 nm respectively. The average heights of the nanodots were varied in the range between 6-9 nm as measured by ellipsometery and cross-section TEM. The density of the nanodots on the substrate is measured approximately 1.1×10^{11} and 4.2×10^{10} nanodots cm^{-2}. The nanodots films were robust and images shown in Figure 4b and d were taken following exposure to ethanolic and hydrogen peroxide for several hours and no significant changes could be observed. XPS can be used to show that the stoichiometry of these dots is Fe_3O_4.
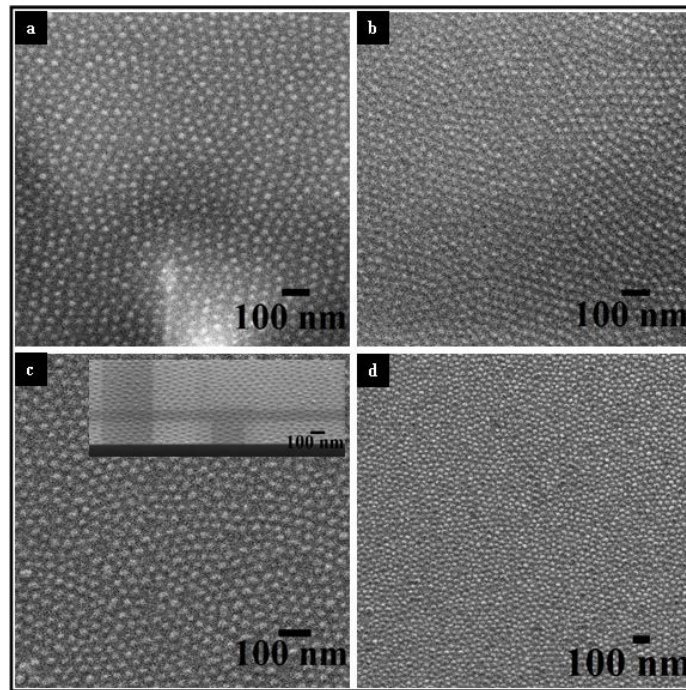

Figure 4. Top-down SEM images of nanodots before and after electrochemical analysis. (a and c) Fe_3O_4 dots fabrication on ITO substrates after UV/Ozone of PS-*b*-PEO 32-11 and PS-PEO 42-11.5. (b and d) Fe_3O_4 dots after electrochemical analysis which proves the stability of dots of sample A and sample B.

Similar data could be recorded for silver nanodots on glass substrates (Figure 5). Well-arranged nanodots were achieved for all three molecular weights of BCP but illustrative data are shown for the PS-b-PEO 42-11.5 (0.6 wt% silver nitrate-ethanol solution used for spin-coating inclusion) sample only. Somewhat surprisingly, the silver is present as metal rather than oxide. This was seen over a range of UV-ozone treatment times except when very extended periods were used. XRD (Figure 5) confirms the presence of silver phases and no crystalline oxide phases were observed. The diffractogram displayed only two features at 2θ angles of 38.02° and 43.58° corresponding to the (111) and (200) reflections of the expected silver face-centred-cubic structure (JCPDS file No. 04-0783) of the metal. EDAX data (insert Figure 5) also suggests high sample purity of the nanodots (sub 10 ppm impurities). The presence of reduced oxide and metal phases does not appear to be unusual from this methodology despite ozone being a good oxidizing agent.[15,16] The reason for reduced phases, including the formation of Fe_3O_4 seen above, appears to be because of the mechanism of polymer matrix decomposition affected by the treatment. The UV degradation of the polystyrene will produce strongly reducing organic radicals as well as carbon monoxide[17] and it would appear that this results in a highly reducing

atmosphere as the silver nitrate decomposes. Further, silver nitrate is well known to decompose to the metal even in oxidizing conditions.

3.2 Electrochemical sensing

The Fe_3O_4 nanodot-ITO substrates were applied as electrochemical sensor for ethanol detection. Comparison of the electrochemical behaviour for the PS-*b*-PEO (32-11) and PS-*b*-PEO (42-11.5) samples are shown in Figure 6. Neither sample exhibit any redox peak in the buffer solution and a scan rate of 50 mV/s. After addition of 0.1 M EtOH, two well defined redox peaks were observed at 0.16 V and -0.4 V for PS-b-PEO 32-11. Smaller oxidation potentials were noted for the lower molecular weight derived samples consistent with enhanced electrocatalytic efficiency towards EtOH oxidation. The reduction potential of about -0.4 V for the PS-b-PEO 32-11 sample is also lower than the literature values.[14] The enhanced responses of these samples and low redox potentials are consistent with the high surface area and density of the nanodots.
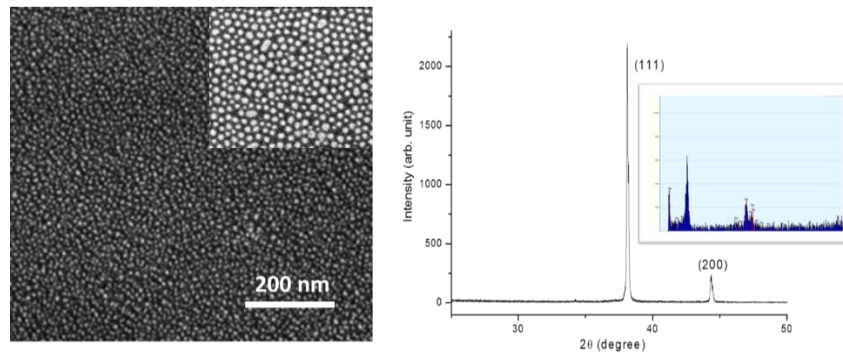

Figure 5. Left, SEM image of silver nanodots samples as described in text. Inset is a magnified image. Right, XRD and EDAX data of same.
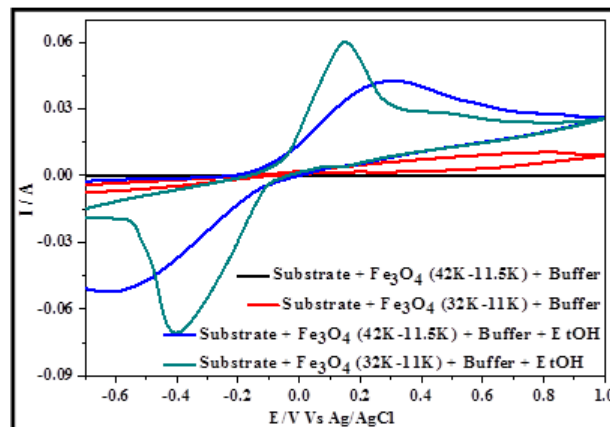

Figure 6. Comparative cyclic voltammograms (CVs) showing the current response of sample PS-b-PEO 32-11 and 42-11.5 to 0.1 M EtOH (phosphate buffer solution, pH = 7.4, scan rate of 50 mV/s).

Figure 7a shows the cyclic voltammograms (CVs) of the PS-b-PEO 32-11 derived sample for a range of EtOH concentrations so that the electrode performance can be assessed. In the forward sweep of oxidation potential there is an increase in peak current from 0.025 A to 0.060 A as the ethanol concentration increases. Figure 9b shows that the catalytic current varies linearly as a function of the EtOH concentration across a range of 0.02-1.0 M. The linear regression equation describing the variation of peak current with concentration has a correlation coefficient (R^2) of

0.99414. The detection limit was calculated as 5.52 mM and the sensitivity of the electrode sample A is 0.039 µA/mM. For the same sample, CV scans were repetitively cycled for 50 cycles in 0.1 M EtOH as shown in Figure 7c. Note that only every tenth are shown in the Figure for clarity. Note that there was a slight increase in current of about 1.3% between first and second scans suggestive of some sample cleaning during the first CV scan. After this no significant changes occurred. These data show the robustness of the samples and their applicability for general laboratory use as a quantitative tool for ethanol detection.
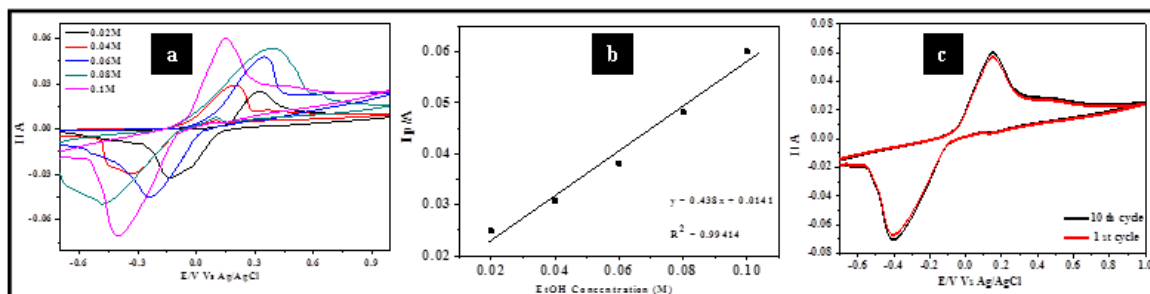

Figure 7. (a) Comparative cyclic voltammograms showing the current response of sample A in phosphate buffer solution, pH =7.4, at different concentrations of EtOH at a scan rate of 50 mV/s. (b) Plot of Ip vs concentration of EtOH. (c) Multiple, repeat scanning of sample A in 0.1 M EtOH in the same conditions as (a).

3.3 Antimicrobial surface properties

The potential of these materials as antimicrobial surfaces is demonstrated here.[18] Illustrative results of the diffusion-type assay method using Ag nanodots obtained using PS-b-PEO 102-34 against *P. fluorescens* and *S. aureus* compared to control samples is shown in Figure 8. These microbials were representative of a series of tests and were chosen as generic tests of antimicrobial efficacy representing gram negative and gram positive types respectively. In Figure 8, clear activity can be observed. The absence of clear zone surrounding the control sample indicated that there were no inhibitory effects towards the microorganism tested, whilst the presence of inhibition zone (clear zone) for the Ag containing substrates indicated antimicrobial activity against the tested microorganism and was clearly visible for the silver nanodots samples. It should also be noted that Ag generally has a greater antimicrobial activity against Gram-negative bacteria than Gram-positive bacteria.[19] The inhibition zone varied considerably with silver loading (as weight % silver in ethanol) and also the molecular weight of the polymer used. Indicative results are shown in Table 1. As can be seen the activity of the samples increases with silver loading suggesting surface concentration is important.

Table 1. The influence of different number of coatings, concentrations of silver precursor and M_n PS-b-PEO to the inhibition zone obtained against *P. fluorescens* and *S. aureus*.

Microorganism Sample[a]	*P. fluorescens*[b]	*S. aureus*[b]
0.4/32-11	74.55	34.29
2.0/32-11	418.72	366.97
4.0/32-11	533.13	401.21
0.4/42-11.5	85.68	45.88
2.0/42-11.5	335.61	286.37
4.0/42-11.5	434.13	327.67
0.4/102-34	82.92	51.12
2.0/102-34	385.45	290.26
4.0/102-34	432.91	386.98

[a]Sample indicated as Ag precursor concentration/polymer mol. weight in kg/mol
[b]Inhibition zones in mm^2

Trends with molecular weight are not obvious in Table 1. This is because increasing the silver precursor concentration has strong effects on the nanodots dimensions, i.e. a 0.4 wt% loading on the smallest molecular weight will not result in the same effect as on the largest molecular weight samples. To fully probe molecular weights, the silver concentration used was optimized to give a selected nanodots diameter range whilst maintaining the height of the nanodots. Clear effects of nanoparticle size on antimicrobial activity have been reported[20] but the very well defined nature of these samples may allow inconsistencies in previous work based on size and shape dispersion to be addressed. Here we focus on the antimicrobial activity of a well-patterned Ag nanodots of different particle sizes (10, 18 and 28 nm and further details in Table 2) obtained using the optimal concentration. These samples were tested using *in vitro* test assays of a diffusion-type assay (Table 2). The results indicated that there was no significant difference in the antimicrobial activity of the Ag nanodots films obtained using PS-b-PEO 42-11.5 and 102-34 as a template; however, a significant increase in the antimicrobial activity was observed for the PS-b-PEO 42-11.5 and 102-34 compared to the lowest molecular weight system. The reason for this appears to be related to surface coverage. Using a hexagonal geometry, the measured nanodots size and the domain spacing, the % coverage of the surface can be calculated as shown in Table 2. It is clear that the greatest contribution to antimicrobial activity is the surface coverage and strongly suggests that size effects in this regime are limited. This might be expected as the bacterial inhibition zone in solid phase assay is defined by the release of Ag^+ from the surface of the substrate.[21]
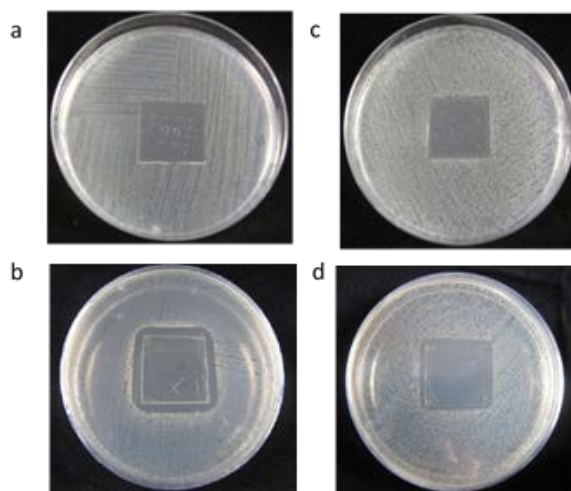

Figure 8. Inhibition zones of a) and c) control sample, b) and d) Ag nanodots PS-b-PEO102-34 with 4% $AgNO_3$ against *P. fluorescens* and *S. aureus,* respectively.

Table 2. Effects of the concentration of silver precursor and average particle size of Ag nanodots manufactured using different M_n PS-b-PEO on the antimicrobial activity (inhibition zone) against *P. fluorescens* and *S. aureus.*

Sample	$AgNO_3$ (w/w) %	Average size (nm) /surface coverage (%)	*P. fluorescens* Inhibition zone[1]	*S. aureus* Inhibition zone[1]
Control	N/A	N/A	0	0
32-11	0.4	10/8.86	74.12 ± 16.31	34.18 ± 9.55
42-11.5	0.6	18/16.66	266.43 ± 2.18	113.25 ± 6.99
102-34	1.2	28/16.84	289.33 ± 6.86	161.84 ± 13.05

[1] Inhibitory zone, measured diameter in mm^2.

* Test was carried out in triplicate.

4. CONCLUSSIONS

It should be clear from these results that block copolymer based methods might represent a platform technology for creating nanosized patterns of different materials on substrate surfaces. In this paper we have outlined methods based around a solvent mediated inclusion method. There are several key advantages of the technique. Firstly, it can be used to create a wide range of oxide[22], complex oxides[23] and metals (as here) but with more sophisticated post-processing, one might imagine the development of many other types of materials. The materials can be created in nanodimensioned form and of highly controlled size and shape and films can demonstrate much larger effective surface areas than planar films. These highly defined patterns can be created without the use of any lithographic methods or expensive post treatments such as reactive ion etching. Whilst absolute periodicity and defect control is not shown here, many applications do not require this sort of precise control and techniques such as directed self-assembly via graphoepitaxy or chemiepitaxy can be used to confer this sort of control.[24] Further, although we have used conventional spin-coating as a deposition method, these films may be realized by other film forming techniques such as dip-coating[25] and these can techniques can be applied to monolithic objects of complex shapes. One can also imagine them being applied to very large surface areas using e.g. roll-to-roll methods as described by Singh et al.[26]

This, it is asserted that block copolymer nanopatterning should be seen as a general thin film, materials technique. It can realize materials difficult to form by conventional deposition techniques or require complex sources and chambers. There are hosts of ferroelectric, ferromagnetic, piezoelectric materials that can be formed rather easily using these methods. The challenge is identifying the most valuable areas to be researched. Conventionally, nano- and micro-patterning follows a procedure where a coherent film is deposited and this is then patterned. There are difficulties in producing the required degree of coherence. Because of lattice mismatches and material chemistries (e.g. mixing, segregation, reaction) either interfacial layers might need to be developed or barrier layers deposited. Either wet or dry etching used to then pattern the layers can also result in stoichiometry changes of the materials or change surface compositions. Strain in some films can cause cracking, damage and delamination. The techniques described here can be used to avoid many of these problems and afford means to prepare uniquely tailored films and coatings.

There are, thus, a host of applications that might be suited to materials developed in this way. This includes catalysis (although bulk particle modification is probably not practical at this time) and in particular technologies requiring catalytic seeds or engineered surfaces, photocatalysis, environmental remediation, magnetic devices, membrane technologies, chromatography etc. We have chosen to illustrate two diverse applications is sensors and antimicrobial surfaces. Clearly, ethanol sensing is important in terms of environmental control, ethanol production and alcohol detection/control. It should be noted that sensitivity to a particular chemical can be engineered by simple change of the nanodots used. The technique gives high sensitivity because of the effective high surface area of the modified surface. The electrodes produced are physically and chemically robust and extremely stable. The methods are cost-effective and it is relatively simple to imagine these materials being integrated into membranes to combine size selective properties with detection capability.

In terms of the antimicrobial properties, highly effective antimicrobial surfaces have been created using these methods. Again, the properties seem to be enhanced because of the large surface areas which allow rapid release of silver ions. Silver nanoparticle based methods have been realized many times and, indeed, have been used in food packaging to increase storage and shelf life.[27] The advantage here is not in the materials properties but instead in the amount of silver that is used. The use of silver nanoparticles because of their inherent toxicology in food applications within the EU is restricted and a safety limit of Ag^+ concentrations < 0.05 mg Ag/kg has been suggested and it is thought that EU consumers have a low acceptability to these products.[28] The use of silver nanoparticles in these applications is normally affected by inclusion of the particles into a polymer matrix limiting the effective surface concentration and inducing mass transport effects. Thus, amounts are relatively high and silver concentrations are of the order of wt%.[29] In this way, these systems can deliver the required properties at loadings orders of magnitude less than conventional systems.

We thus hope that this article provides an argument for the widespread application of these techniques across a number of industry sectors. We have only presented one possible preparation methodology and techniques such as pattern

transfer, vapor phase inclusion, direct deposition have not been considered. It is hoped and expected that similar application will be developed over the next few years and the methods become the generic way of generating patterned surfaces.

REFERENCES

[1] G. M. Whitesides and B. Grzybowski, "Self-assembly at all scales, Science", 295, pp. 2418-2421, 2002.

[2] R. A. Farrell, N. Petkov, M. A. Morris and J. D. Holmes, "Self-assembled templates for the generation of arrays of 1-dimensional nanostructures: From molecules to devices", J. Coll. Interface Sci., 349, pp. 449-472, 2010.

[3] Y. S. Lee, Self-assembly and nanotechnology systems: design, characterization, and applications, J Wiley and Sons, Hobroken, New Jersey, 2011.

[4] W. Lu and A. M. Sastry, "Self-assembly for semiconductor industry", IEEE Trans. Semiconductor Manufacturing, 20, pp. 421-431, 2007.

[5] International Technology Roadmap for Semiconductors, "Emerging research materials", 2013. http://www.itrs.net/Links/2013ITRS/2013Chapters/2013ERM.pdf.

[6] R. A. Farrell, T. G. Fitzgerald, D. Borah, J. D. Holmes and M. A. Morris, "Chemical interactions and their role in the microphase separation of block copolymer thin films", J. Mol. Sci., 10, pp. 3671-3712, 2009.

[7] S-J Jeong, J. Young Kim, B. Hoon Kim, H-S. Moon, S. Ouk Kim, "Directed self-assembly of block copolymers for next generation nanolithography, Materials Today 16, pp. 468–476, 2013.

[8] H. Wang, K-Q. Zhang, "Photonic crystal structures with tunable structure color as colorimetric sensors", Sensors, 13, pp. 4192-4213, 2013.

[9] H. Zhao, W. Gu, E. Sterner, T. P. Russell, E. B. Coughlin and P. Theato, "Highly ordered nanoporous thin films from photocleavable block copolymers", Macromolecules, 44, 6433–6440, 2011

[10] M. Hillmyer, "Nanoporous membranes from block copolymer precursor", Adv. Poly. Sci., 190, pp. 137-181, 2008.

[11] P-H. Tung, S-W. Kuo, K-U. Jeong, S. Z. D. Cheng, C-F. Huang F-C. Chang, "Formation of honeycomb structures and superhydrophobic surfaces by casting a block copolymer from selective solvent mixtures", Macromolecular Rapid Communications, 28, pp. 271–275, 2007

[12] R. A. Farrell, N. T. Kinahan, S. Hansel, K. O. Stuen, N. Petkov, M. T. Shaw, L. E. West, V Djara, R J. Dunne, O. G. Varona, P. G. Gleeson, S-J. Jung, H-Y Kim, M. M. Koleśnik, T Lutz, C. P. Murray, J. D. Holmes, P. F. Nealey, G. S. Duesberg, V. Krstić and M. A. Morris, "Large-scale parallel arrays of silicon nanowires via block copolymer directed self-assembly", Nanoscale, 4, pp. 3228-3236.

[13] S. Rasappa, D. Borah, C. M. Faulkner, T. Lutz, M. T. Shaw, J.D. Holmes and M. A. Morris, "Fabrication of a sub-10 nm silicon nanowire based ethanol sensor using block copolymer lithography", Nanotechnology, 24, 065503, pp. 1-8, 2013.

[14] S. Rasappa, D. Borah, R. Senthamaraikannan, C. Faulkner, J. D. Holmes, M. A. Morris, "Fabrication of 3-D nanodimensioned electric double layer capacitor structures using block copolymer templates", Journal of Nanoscience and Nanotechnology, 14, pp. 5221-5227, 2014.

[15] T. Ghoshal, T. Maity, J. F. Godsell, S. Roy and M. A. Morris, "Large scale monodisperse hexagonal arrays of superparamagnetic iron oxides nanodots: a facile block copolymer inclusion method", Adv. Mater., 24, pp. 2390-2397, 2012.

[16] T. Ghoshal, T. Maity, R. Senthamaraikannan, M. T. Shaw, P. Carolan, J. D. Holmes, S. Roy, M. A. Morris, "Size and space controlled hexagonal arrays of superparamagnetic iron oxide nanodots: magnetic studies and application", Sci. Rep. 3, 2772, pp. 1-8, 2013.

[17] E. Yousaf and R. Haddad, "Photodegradation and photostabilization of polymers, especially polystyrene: review", SpringerPlus, 2, pp. 398-440, 2013.

[18] M. A. Morris, J. Kerry, M. Cruz, E. Cummins and T. Ghoshal, "An antimicrobial food package", International (PCT) Application No. PCT/EP2013/06371 published as WO2014/001541, 2014.

[19] S. Shrivastava, T. Bera, A. Roy, G. Singh, P. Ramachandrarao and D. Dash, "Characterization of enhanced antibacterial effects of novel silver nanoparticles", Nanotechnology, 18, 225103, 2007.

[20] M. C. Cruz-Romero, T. Murphy, M. Morris, E. Cummins and J. P. Kerry, "Antimicrobial activity of chitosan, organic acids and nano-sized solubilisates for potential use in smart antimicrobially-active packaging for potential food applications", Food Control, 34, pp. 393-397, 2013.

[21] Z. Li, D. Lee, X. Sheng, R. E. Cohen, M. F. Rubner, "Two-level antibacterial coating with both release-killing and contact-killing capabilities", Langmuir, 22, pp. 9820-9823, 2006.

[22] T. Ghoshal, P. G. Fleming, J. D. Holmes and M. A. Morris, "The stability of "Ce2O3" nanodots in ambient conditions: A study using block copolymer templated structures", Journal of Materials Chemistry, 22, pp. 22949-22958, 2012.

[23] J. Varghese, T. Ghoshal, N. Deepak, C. O'Regan, R.W. Whatmore, M.A. Morris and JD Holmes "Fabrication of arrays of lead zirconate titanate (PZT) nanodots via block copolymer self-assembly", Chemistry of Materials 25, pp. 1458-1463, 2013

[24] B. H. Kim, J. Y. Kim and S. O. Kim, "Directed self-assembly of block copolymers for universal nanopatterning", Soft Matter, 9, pp. 2780-2786, 2013.

[25] S. Roland, C. Pellerin, C. G. Bazuin,* and R.E. Prud'homme, "Evolution of small molecule content and morphology with dip-coating rate in supramolecular PS−P4VP thin films", Macromolecules, 45, pp. 7964−7972, 2012.

[26] G. Singh, S. Batra, R. Zhang, H. Yuan, K. G. Yager, M. Cakmak, B. Berry and A. Karim, "Large-scale roll-to-roll fabrication of vertically oriented block copolymer thin films", ACS Nano, 7, pp 5291–5299, 2013.

[27] A. Martinez-Abad, J. M. Lagaron, M. J. Ocio, "Development and characterization of silver-based antimicrobial ethylene-vinyl alcohol copolymer (EVOH) films for food-packaging applications", J. Agric. Food Chem., 60, pp. 5350-5359, 2012

[28] A. Fernández, E. Soriano, G. López-Carballo, P. Picouet, E. Lloret, R. Gavara, P. Hernández-Muñoz, "Preservation of aseptic conditions in absorbent pads by using silver nanotechnology", Food Res. Int., 42, pp. 1105-1112, 2009.

[29] K. Ghosh, S. N. Maiti, "Mechanical properties of silver-powder-filled polypropylene composites", J. Appl. Polymer Sci., 60, pp. 323-331, 1996.